Methanol diffusion and relaxation in uniaxially drawn poly(ether sulphone)

C. C. Chau, D. L. Fear and R. A. Wessling
The Dow Chemical Company, M. E. Pruitt Research Center, Central Research, Midland, MI 48674, USA
(Received 11 May 1988; revised 19 December 1988; accepted 27 January 1989)

Poly(ether sulphone) was uniaxially drawn at 255°C and quenched to temperatures below T_g to produce a stabilized neck. The rate of penetration of liquid methanol in the necked region was faster than in the undeformed material. The kinetics were combinations of Fickian and case II. Both the resolved diffusivity and case II velocity constant increased with draw ratio up to 2.27. The diffusivity and velocity constant did not seem to vary with the strain rate of drawing from 0.033 to 0.67 min^{-1}. At later stages of sorption, localized cracks developed along the draw direction. Sorption in the undeformed material did not cause apparent cracking. The contribution of relaxation to the total flux across the thickness increased with draw ratio and that of diffusion decreased. These observations indicate that drawing facilitates the transport of liquid methanol resulting from enhanced matrix relaxation.

(Keywords: methanol; diffusion; relaxation; drawing; poly(ether sulphone))

INTRODUCTION

The transport of small molecules in polymers is known to be affected by the mechanical history of the material. This effect can be manifested by the variations of transport kinetics, the equilibrium solubility, the dimensional changes and/or deformation caused by the swelling stress. Earlier studies have indicated that the behaviour varies dramatically with the nature of the material. For semicrystalline polymers, predeformation usually impedes the sorption or transport process, resulting in slower rate of penetration or reduced solubility. These were demonstrated by transport of both organic and gas molecules in uniaxially drawn polyethylene[1–7], polypropylene[8,9] and other materials[10–12]. The structure of the deformed material can sometimes be altered by solvent-induced crystallization[13–15], and therefore dimensional changes are often found.

The behaviour for glassy polymers is rather different. Deformation was found to cause reduced sorption and diffusion when the direction of transport is normal to the chain orientation in some cases and enhanced response in others. This effect was demonstrated by methanol sorption in compressed[16] poly(methyl methacrylate) (PMMA) and in the shear bands of PMMA[17], in which the transport of liquid methanol was faster in the deformed material. Windle[18] found that the same process was retarded when tensile strain was introduced normal to the penetration front. Uniaxially oriented polystyrene, however, showed different behaviour; the rate of penetration of hexane[19] was found to increase with draw ratio. Solvent-induced relaxation or crazing is often observed. Typical examples were solvent crazing in oriented polystyrenes[19,20]. So far these studies have been mainly focused on determining the influence of the deformation or orientation on transport, with little emphasis on mechanistic understandings.

As a continued effort towards the understanding of orientation effects on transport in glassy polymers, poly(ether sulphone) (PES), an amorphous polymer with a relatively high glass transition temperature, was studied. PES is a tough, rigid, high-strength thermoplastic suitable for a wide range of engineering applications[21]. A study of the transport behaviour in oriented PES could help in revealing the microdeformation process during orientation. Liquid methanol, a non-solvent but perhaps a suitable swelling agent for PES, was chosen for detecting the uniaxial drawing effect. Earlier, the sorption and swelling behaviour of methanol and other solvents in PES were studied by Ghavamikia and Blackadder[22]. These authors observed non-Fickian behaviour with little comments on the mechanism of transport. In this study, the sorption behaviour of uniaxially drawn PES was compared with that of the undeformed material. The kinetics of transport were analysed in terms of both diffusion and relaxation. Solvent-induced deformation in drawn samples was observed and the possible mechanisms are discussed.

EXPERIMENTAL

Materials and specimen preparation

The poly(ether sulphone) used in this study was ICI Victrex 3600 G resin. It has a glass transition temperature of 226°C as determined by differential scanning calorimetry (heating rate 10°C min^{-1}). The material, received in pellet form, was dried in a vacuum oven at 100°C for 24 h. It was compression moulded at 310°C in a Pasadena hydraulic press into 0.8–0.9 mm thick sheets by using thickness moulding gauges with 3 min preheating, 6 min moulding under 10000 psi and 10 min cooling with circulating water. Standard tensile test specimens with a gauge length of 1.5 inch and a width of 0.5 inch were cut from the sheets with a steel ruled die. They were annealed at 200°C for 3 h and air cooled to room temperature.

Instron tensile drawing

Specimens were stretched in an Instron tensile test machine with a Thermotron oven. The oven was preheated to 255°C as indicated on a temperature recorder with

0032-3861/89/112087-07$03.00
© 1989 Butterworth & Co. (Publishers) Ltd.

the thermocouple located near the jaws. The specimen was loaded on the jaws enclosed in the oven and thermally equilibrated at the set temperature for 15 min. The specimen was then stretched at a constant crosshead speed to a preset total elongation. A jet of cold water was then instantly sprayed onto the specimen from a nozzle connected to a tubing line built in the oven. The spraying was controlled manually outside the oven. The temperature in the oven was rapidly dropped to below 200°C after the spray quenching. The specimen was then removed from the oven with the drawn dimensions. Specimens were stretched with various strain rates and total elongations to develop uniform necks. The shape and uniformity of the neck varied with the strain rate and total elongation used. Higher strain rates usually produced more uniform necks. The neck size and uniformity decreased moderately with the increase of total elongation. Tests were repeated to provide a selection of stretched bars for sorption tests. Samples 25 mm long were razor-cut from the most uniform portion of the neck of the stretched specimens. The cross-sectional dimension varied with the stretching parameters used. The dimensions of the cut sample were measured.

Density measurements

Additional samples were cut from the drawn necks for density measurements. The densities were measured in a density gradient column containing aqueous zinc bromide solutions. The column was maintained at 25°C by enclosing in a constant-temperature water jacket. The density gradient was indicated by floats, which have known densities with resolution of four decimal points. The positions of specimens were measured by using a cathetometer as soon as samples were stabilized in the column, usually within 10 min of immersion. To avoid any possible swelling or solvent crazing effect, all measurements were made within 15 min of immersion. The densities of specimens were calculated by interpolation.

Methanol sorption studies

The cut samples were put into methanol-filled glass bottles of 18 mm diameter, 50 mm long, which were kept in a Fisher Isotemp Series 200 forced convection oven. The oven was modified by installing a model 2002 process controller made by LFE Corp., capable of controlling and resolving 0.1°C for precise control of the oven temperature. The original temperature controller was used as the high limit. The temperature was indicated by digital readout. The sorption study was conducted by measuring the weight gain of the sample periodically. Samples were removed from the solvent, blotted on Kim-Wipe tissues, weighed in a Mettler H35AR digital balance, capable of resolving 0.1 mg, and returned immediately to methanol for another period of immersion. Undeformed PES samples with a uniform dimension of 25 mm × 12.5 mm × 0.8 mm were also prepared for the sorption test. They were made by following the same preparation method as described previously. The cut samples were polished on Emery papers to No. 400 grit finish to smooth out the cut surfaces and then annealed at 200°C for 3 h. Samples were then furnace cooled to room temperature over a 5 h time period.

Electron microscopy

Some samples were dried in air for 24 h and vacuum coated with a thin layer of gold by using a Polaron E5200 vacuum sputtering apparatus. Samples were then examined under an ISI DS-130C scanning electron microscope using a 10 kV operating voltage.

RESULTS AND DISCUSSION

Uniaxially drawn poly(ether sulphone) specimens

Specimens produced by uniaxial drawing appear to be transparent with light drawing marks or striations on the surface as observed under SEM. The degree of drawing is represented by a draw ratio, obtained from the ratio of drawn length divided by the gauge length of the specimen. The draw ratio (*DR*) was varied from 1 to 2.27. Above the draw ratio of 2.27, necks of uniform dimension were not obtainable. The drawn specimens seem to show structural variations as indicated by the density measurements. As shown in *Figure 1*, the density decreases slightly when the draw ratio is higher than 1.43. The extent of decrease, however, was within 1%.

The kinetics of methanol transport

Preliminary experiments showed that the sorption rate was very low at room temperature. Further studies were conducted at elevated temperatures. The sorption data are presented as fractional weight gain (amount of sorption at any time t/equilibrium amount of absorption) as a function of time. The sorption kinetics of both the undeformed and the deformed samples stretched with a strain rate of 0.067 min^{-1} at 50°C are shown in *Figure 2*. The sorption rates in the deformed samples are higher than that of the undeformed samples. The sorption rate appears to be increasing with increase in the draw ratio from 1.43 to 2.27. At later stages of sorption, cracks developed in the drawn samples. The formation of cracks and their effect on weight-gain measurements are discussed later. The weight-gain percentage does not increase linearly with time in all cases, indicating that simple case II[23] behaviour was not followed. Examination of the data by plotting the weight-gain percentage against $\sqrt{t}$ indicated that a simple Fickian diffusion behaviour was not obeyed either (not shown). The kinetics are therefore probably mixed processes of diffusion and case II type of relaxation, as could occur with large penetrants or penetrants with high solution concentrations.

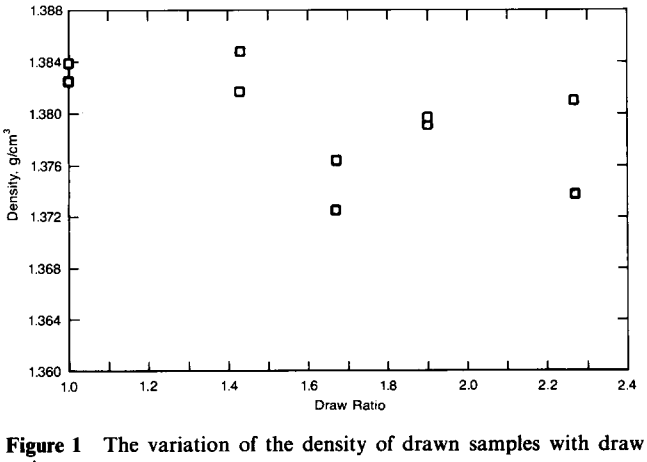

Figure 1 The variation of the density of drawn samples with draw ratio

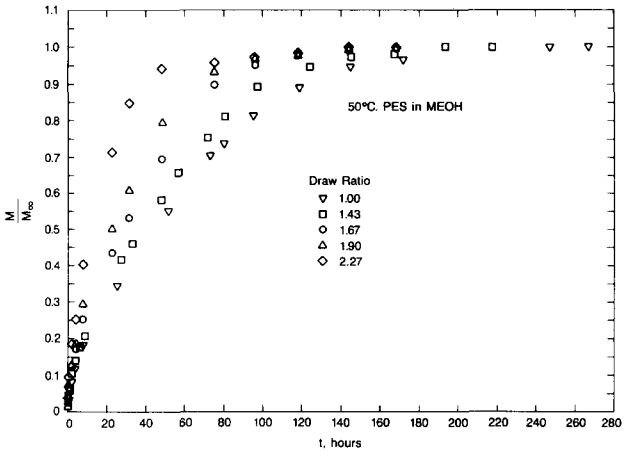

Figure 2 The sorption kinetics of methanol into both undeformed and drawn (strain rate 0.067 min^{-1}) PES samples at 50°C

The sorption results were then analysed by considering both diffusion and relaxation in the matrix. For a finite slab in which transport occurs from both faces, Wang *et al.*[24] and Wang and Kwei[25] proposed a simple simultaneous diffusion and case II transport model by assuming a constant diffusivity (D) and a velocity constant (v) for the transport. A modified model taking into account the diminishing flux and concentration gradient towards the middle plane was provided by Li[16]. The general flux equation can be expressed as follows:

$$J = -D\frac{\partial C}{\partial x} + v(C - C_0) \tag{1}$$

The concentration distribution in the slab of thickness $2l$ at time t is:

$$\frac{C}{C_1} = 1 - 2\exp\left(-\frac{v(l-x)}{2D}\right) \times \sum_{n=1}^{\infty} \frac{\lambda_n \sin[\lambda_n(l-x)/l]}{\beta_n^2[1-(2D/vl)\cos^2\lambda_n]} \exp\left(-\frac{\beta_n^2 Dt}{l^2}\right) \tag{2}$$

where C is the concentration of the penetrant, C_0 is the concentration in the middle plane, and v is the velocity component of the penetrant, which is caused by case II polymer relaxation, and is in the direction of flux. It is a negative constant used in equation (2). C_1 is the surface concentration, x is the distance measured from the middle plane ($0 < x < l$). λ_n are positive roots of:

$$\lambda_n = \frac{vl}{2D}\tan\lambda_n \tag{3}$$

and β_n is related by λ_n by:

$$\beta_n^2 = \frac{v^2 l^2}{4D^2} + \lambda_n^2 \tag{4}$$

The total absorption M at any time t was found to be:

$$\frac{M}{M_\infty} = 1 - 2\sum_{n=1}^{\infty} \frac{\lambda_n^2[1-2\cos(\lambda_n)\exp(-vl/2D)]}{\beta_n^4[1-(2D/vl)\cos^2\lambda_n]} \times \exp\left(-\frac{\beta_n^2 Dt}{l^2}\right) \tag{5}$$

where M_∞ is the equilibrium amount of absorption corresponding to the solubility of the penetrant.

By using a simulation program described elsewhere[26] and adjusting the value of D and v, equation (5) was found to fit the sorption data well at least for the initial (60% sorption) portion of the process. Shown in *Figure 3* are the fits for an undeformed and a drawn ($DR = 1.90$) sample. The fitted D and v are plotted in *Figure 4* as a function of draw ratio. Both D and v increased apparently with draw ratio with a maximum increase of about two-fold. This result indicates that uniaxial drawing of PES could have opened up the structure, thus facilitating the movement of penetrating species. The behaviour is similar to that of methanol in amorphous PMMA[16] in which compression appeared to have eliminated the rate-limiting step of transport. It is, however, different from that in the drawn materials[18], in which the transport process was impeded perpendicular to the draw direction.

To see how the strain rate affects the transport behaviour, the samples were prepared by drawing at different crosshead speeds to reach 1 inch total elongation. The drawn samples had about the same dimension within the strain rate range of 0.033 to 0.67 inch min^{-1}. The necked region of the drawn samples was cut and used for sorption. The sorption data are shown in *Figure 5*.

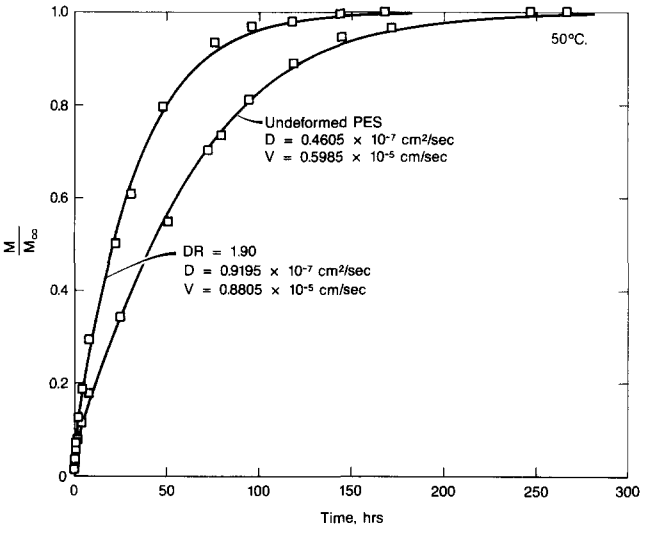

Figure 3 The fit of sorption data by considering simultaneous diffusion and matrix relaxation. The best fit was obtained by properly adjusting D and v using equation (5)

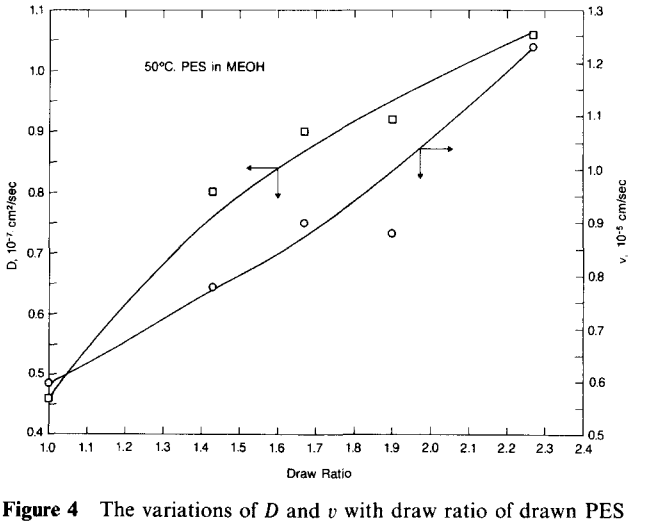

Figure 4 The variations of D and v with draw ratio of drawn PES

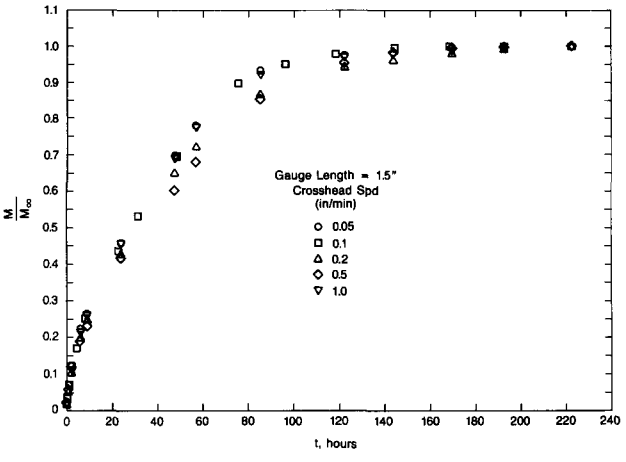

Figure 5 The sorption kinetics of methanol into drawn PES samples prepared by drawing with various strain rates

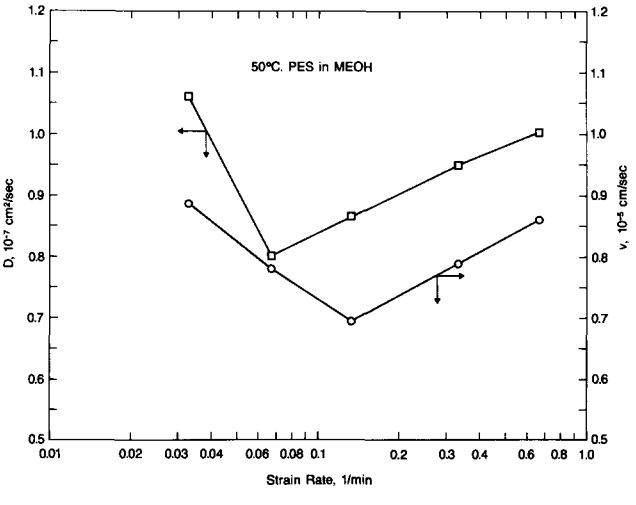

Figure 6 The variations of D and v with the strain rate of drawing for samples drawn at 67% elongation

Again, the results do not follow a simple case II behaviour nor can a systematic trend of the curve with the strain rate of drawing be seen. The resolved diffusivity D and velocity constant v based on equation (5) are shown in *Figure 6*. Both D and v varied within a limited range, with no apparent dependence on the strain rate used. This observation seems to indicate that the rate of drawing for an amorphous polymer such as PES does not change the rate-limiting mechanism during transport. This behaviour is different from that of semicrystalline polymers[9], in which the rate of stretching significantly affected the transport kinetics.

Flux distribution in the drawn sample

To understand further the transport process in the drawn samples, the flux distribution in the slab from contributions of diffusion and relaxation were analysed. As previously reported[9], the positional variation of the concentration profile can be expressed as:

$$\frac{\partial(C/C_1)}{\partial x}=2\exp\left(-\frac{v(l-x)}{2D}\right)\sum_{n=1}^{\infty}\exp\left(-\frac{\beta_n^2 Dt}{l^2}\right)\times\left(\frac{\lambda_n}{l}\right)\frac{\lambda_n\cos[\lambda_n(l-x)/l]}{\beta_n^2[1-(2D/vl)\cos^2\lambda_n]}-\frac{v}{2D}\left(1-\frac{C}{C_1}\right) \quad (6)$$

A similar type of analysis was conducted for the drawn samples. The concentration distribution across the sample thickness and the positional variation of the concentration gradient for constants v and D should behave similarly to that of figures 11 and 12 of a previous publication[9]. The contributions of diffusion and relaxation to the total flux J at any time t were examined for the drawing effect. First of all, the relaxation-flux ratio, i.e. the ratio of the relaxation flux over the total flux, J_v/J_{tot}, for the undeformed PES is plotted against position for various sorption times as shown in *Figure 7*; as understood, the surface region always has a significant contribution due to relaxation. It appears to decrease rapidly towards the centre of the slab. Finally, relaxation terminates at the middle plane ($x/l=0$). The process seems to become more dominating as time increases. Again, this shows that the transport process at the surface region is mostly relaxation-controlled.

To see how the drawn sample behaves, the relaxation-flux ratio at 10 h sorption for samples with various draw ratios is shown in *Figure 8*. It is seen that, as draw ratio increases, the relaxation-flux ratio also increases across the sample thickness, with the maximum increase occurring at the highest draw ratio, 2.27. A slight crossover of the curves is observed at low draw ratios; however, the disparity becomes clearer as the draw ratio increases. On the surface the relaxation seems to be more pronounced as the draw ratio increases. The progressive increase in flux appears to have a similar pattern as that of the time effect as shown in *Figure 7*, indicating that drawing facilitated matrix relaxation and allowed faster movement of the penetrant towards the centre.

The flux contribution due to Fickian diffusion was analysed by the same method. The positional variation of the diffusion-flux ratio, namely the ratio of diffusional flux over the total flux, J_D/J_{tot}, is shown in *Figure 9*. The profile of the curve shows an inverse relationship with that of relaxation. The surface shows a small contribution of diffusion, while the centre is totally diffusion-controlled. As time increases, the diffusional contribution decreases, and the process is presumably taken over by the matrix

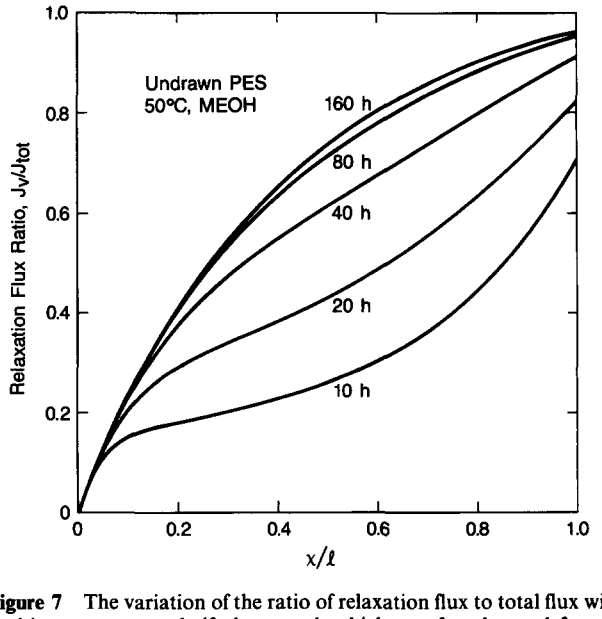

Figure 7 The variation of the ratio of relaxation flux to total flux with position across one-half the sample thickness for the undeformed material at different sorption times

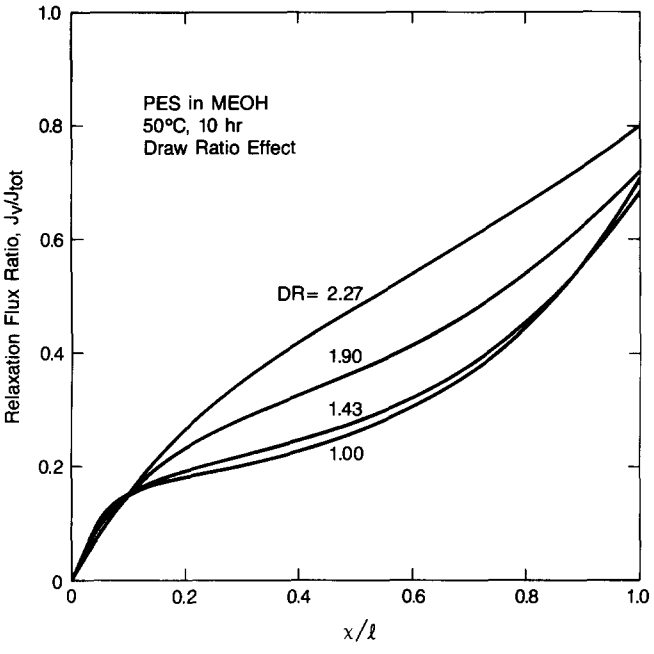

Figure 8 The variation of the ratio of relaxation flux to total flux with position across one-half the sample thickness for the drawn PES samples with different draw ratios

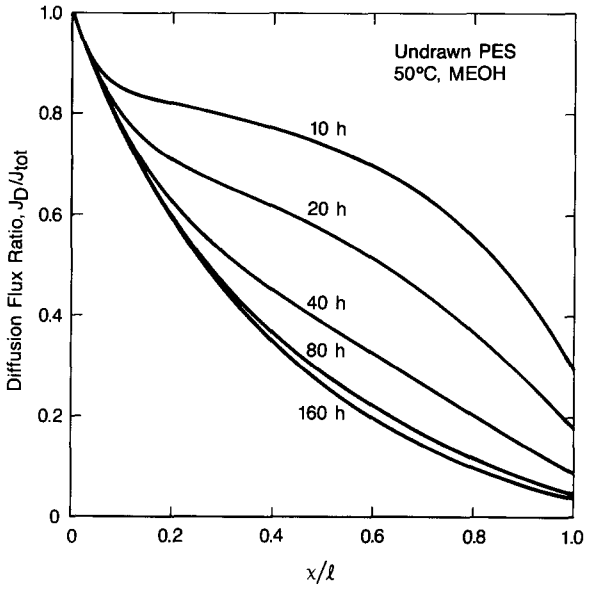

Figure 9 Plots of the ratio of diffusion flux to total flux as a function of position across one-half the sample thickness for the undeformed sample

relaxation. For the drawn sample, the behaviour seems to be similar, as shown in *Figure 10*. The diffusion-flux ratio decreases as the draw ratio increases. On the surface, diffusion seems to be diminishing as draw ratio increases, while the flux at the middle plane appears to be totally due to diffusion. The relationship is just the inverse of that of *Figure 8* for the relaxation-flux ratio. These observations indicate that uniaxial drawing enhances case II type matrix relaxation behaviour and reduces the contribution of Fickian diffusion, though the diffusivity increases with draw ratio. The large contribution of relaxation caused the sorption process to be fast and non-Fickian. As proposed, the case II mechanism was considered as a deformation process occurring at the penetration front. Such deformation may proceed in a relatively easy fashion when an amorphous polymer matrix is oriented in a direction perpendicular to that of transport.

Deformation upon sorption

For undeformed and annealed samples, sorption of methanol did not cause apparent deformation throughout the process. Samples cut without annealing sometimes showed a cracking effect around the cut edges due to the stresses introduced during cutting. At later stages of sorption, crazes or cracks developed in a random fashion as indicated by the reflectivity. This effect, however, was eliminated by annealing before sorption. Sorption in the stretched samples invariably produced cracks. When the total sorption was lower than about 40%, no visible crazes or cracks on the sample surface could be identified even under the optical microscope. When the sorption was higher than 50% of the total absorption, crazes or cracks appeared along the draw direction. The surface morphology of the cracks is shown in *Figure 11*. The cracks appeared as short open segments oriented along the direction of draw. The endings of the cracks were diverted slightly away from the original direction, typical of craze interactions observed in glassy polystyrene[27]. The formation of cracks could affect the sorption measurements at later stages due to additional sorption from crack surfaces. To see how the crack formation affected the weight-gain measurements, the weight was recorded periodically on the balance. The results are shown in *Figure 12* for both an undeformed sample and a stretched sample. The fact that both samples showed the same weight decline with the weighing time indicates that the weight gain recorded for the drawn sample represents the sorption of the matrix. The measurements could, however, include the sorption in the crack-tip crazes or plastic zones, and were not resolvable from the study.

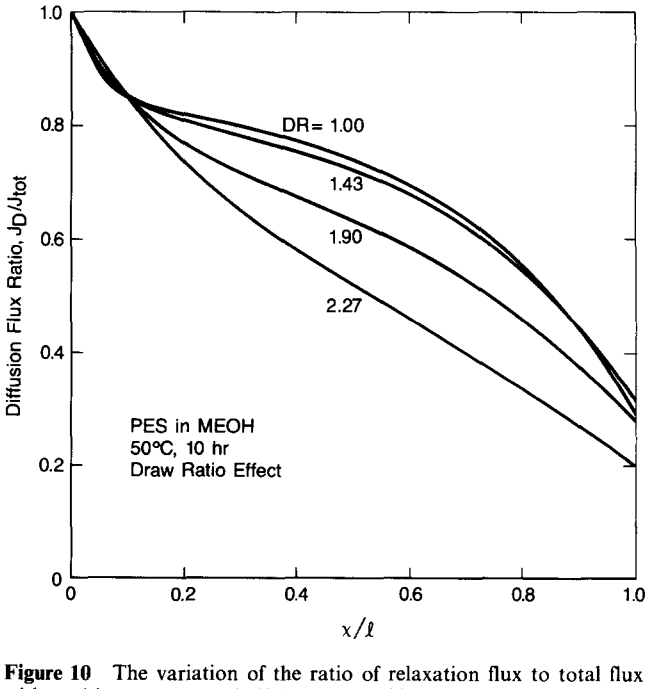

Figure 10 The variation of the ratio of relaxation flux to total flux with position across one-half the sample thickness for the drawn PES samples with different draw ratios

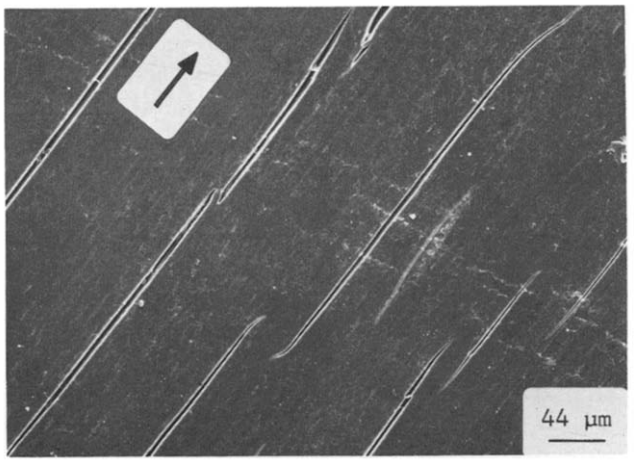

Figure 11 The morphology of cracks developed on the drawn sample upon sorption of methanol (arrow indicates draw direction)

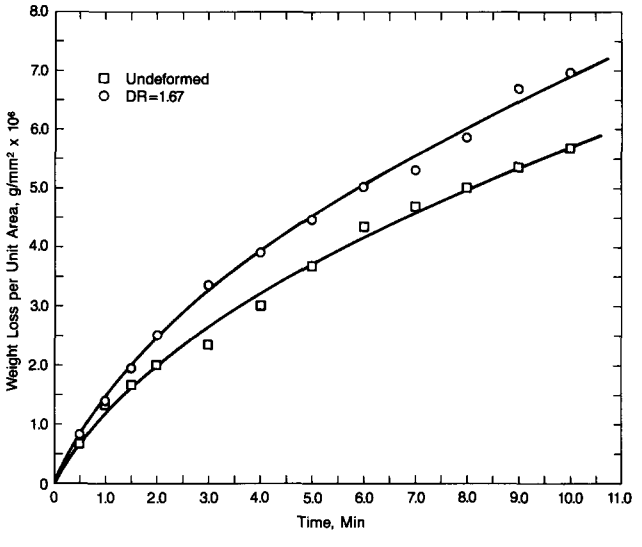

Figure 12 The variations of sample weight with the recording time for samples with and without cracks

The solubility and draw ratio relationship is shown in *Figure 13*. It is clear that drawing increases the solubility of methanol, with a maximum increase of about 14% observed in this study. This observation is different from that of methanol in PMMA[16], in which the solubility did not vary with deformation. The solubility, however, seemed to be independent of the strain rate of drawing, as shown in *Figure 14* for samples drawn to 67% total strain.

The formation of cracks in the drawn sample is of interest. Earlier, the crack formation in solvent-crazed polystyrene containing shear bands[28] was explained by using a dislocation model. In the preparation of PES drawn samples, internal stresses could be developed by cold-water quenching. Since drawing is probably preceded by sliding and rotation of molecular chains along the maximum shear stress direction, the internal stresses can be viewed as produced by intersections of slip lines encompassing the tensile axis, as shown schematically in *Figure 15* with dislocation pile-ups developed at the intersection. The pile-ups eventually developed cracks along the tensile direction with the assistance of swelling stress induced by the sorption of methanol.

SUMMARY AND CONCLUSIONS

The rate of penetration of liquid methanol in drawn PES was faster than in the undeformed material. The kinetics could be represented by a combination of Fickian diffusion and case II relaxation.

The resolved diffusivity and velocity constant increased

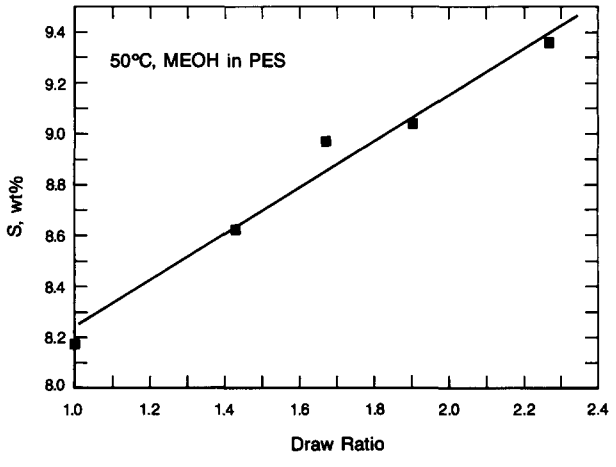

Figure 13 The variation of solubility of methanol in PES with draw ratio

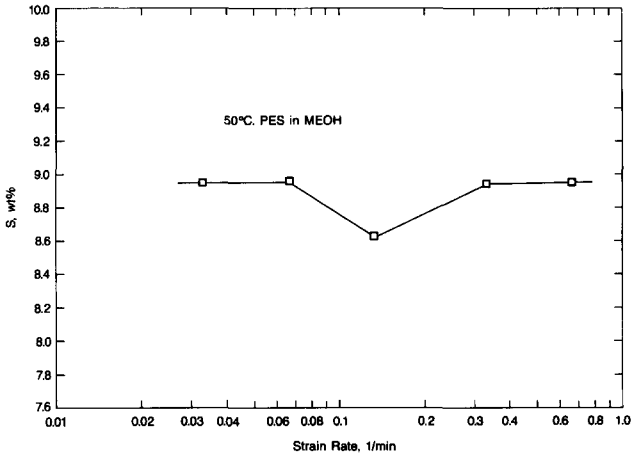

Figure 14 The variation of solubility of methanol in PES with the strain rate of drawing

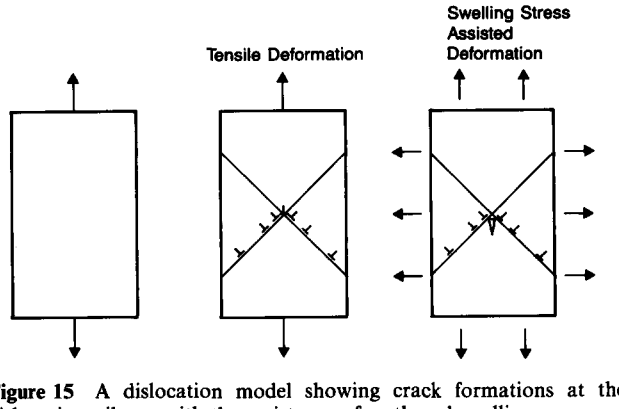

Figure 15 A dislocation model showing crack formations at the dislocation pile-up with the assistance of methanol swelling

with draw ratio with a maximum two-fold increase. They showed no dependence on the strain rate of drawing. The solubility of methanol also increased with draw ratio.

The contribution of relaxation to the total flux across the thickness increased with draw ratio and that of diffusion decreased. Drawing appeared to enhance the matrix relaxation upon sorption of methanol. The diffusional flux became relatively less significant.

Cracks developed along the drawing direction at later stages of sorption. The formation of cracks was attributed to the internal stresses produced by quenching, as explained by using a dislocation model.

ACKNOWLEDGEMENTS

We wish to thank Don Foye for preparing the samples and conducting the drawing experiments, and Ann McNeal for organizing and typing the manuscript. The permission of The Dow Chemical Company to publish the work is deeply appreciated. We would also like to thank the reviewers for their comments on this work.

REFERENCES

1 Peterlin, A., Williams, J. L. and Stannett, V. *J. Polym. Sci.* (*A-2*) 1967, **5**, 957
2 Williams, J. L. and Peterlin, A. *J. Polym. Sci.* (*A-2*) 1971, **9**, 1483
3 Peterlin, A. *J. Macromol. Sci.–Phys.* (*B*) 1975, **11**(1), 57
4 Marshall, J. M., Hope, P. S. and Ward, I. M. *Polymer* 1982, **23**, 142
5 De Candia, F., Russo, R., Vittoria, V. and Peterlin, A. *J. Polym. Sci., Polym. Phys. Edn.* 1980, **18**, 2083
6 Holden, P. S., Orchard, G. A. J. and Ward, I. M. *J. Polym. Sci., Polym. Phys. Edn.* 1985, **23**, 709
7 Holden, P. S., Orchard, G. A. J. and Ward, I. M. *J. Polym. Sci., Polym. Phys. Edn.* 1985, **23**, 2295
8 Choy, C. L., Leung, W. P. and Ma, T. L. *J. Polym. Sci., Polym. Phys. Edn.* 1984, **22**, 707
9 Chau, C. C. and Fear, D. L. *Polym. Eng. Sci.* 1986, **26**, 1533
10 El-Hibri, M. J. and Paul, D. R. *J. Appl. Polym. Sci.* 1986, **31**, 2533
11 Swaroop, N. and Gordon, G. A. *Polym. Eng. Sci.* 1980, **20**(1), 78
12 Brady, T. E., Jabarin, S. A. and Miller, G. W. *ACS Prep., Div. Org. Coat. Plast. Chem.* 1974, **34**(1), 528
13 Jameel, H., Waldman, J. and Rebenfeld, L. *J. Appl. Polym. Sci.* 1981, **26**, 1795
14 Kusuyama, H., Takase, M., Higashihata, Y., Tseng, H. T., Chatani, Y. and Tadokoro, H. *Polymer* 1982, **23**, 1256
15 Ware, R. A., Tirtowidjojo, S. and Cohen, C. *J. Appl. Polym. Sci.* 1981, **26**, 2975
16 Li, J. C. M. *Polym. Eng. Sci.* 1984, **24**, 750
17 Chau, C. C. and Li, J. C. M. *Phil. Mag.* (*A*) 1981, **44**, 493
18 Windle, A. H. *J. Membr. Sci.* 1984, **18**, 87
19 Nicolais, L., Drioli, E., Hopfenberg, H. B. and Apicella, A. *Polymer* 1979, **20**, 459
20 Jacques, C. H. M., Hopfenberg, H. B. and Stannett, V. *J. Appl. Polym. Sci.* 1974, **18**, 223
21 Ballintyn, N. J. in Kirk-Othmer 'Encyclopedia of Chemical Technology', 3rd Edn., Vol. 18 (Eds M. Grayson and D. Eckroth), Wiley, New York, 1982, p. 843
22 Ghavamikia, H. and Blackadder, D. A. *Polymer* 1980, **21**, 901
23 Alfrey, T., Jr, Gurnee, E. F. and Lloyd, W. G. *J. Polym. Sci.* (*C*) 1966, **12**, 249
24 Wang, T. T., Kwei, T. K. and Frisch, H. L. *J. Polym. Sci.* (*A-2*) 1969, **7**, 2019
25 Wang, T. T. and Kwei, T. K. *Macromolecules* 1973, **6**, 919
26 Agin, G. L. and Blau, G. E. *AIChE Symp. Ser.* 1982, **214**, 78, 108
27 Chau, C. C., Rubens, L. C. and Bradford, E. B. *J. Mater. Sci.* 1985, **20**, 2359
28 Chau, C. C. and Li, J. C. M. *J. Mater. Sci.* 1983, **18**, 3047